Topological Edge States with Zero Hall Conductivity in a Dimerized Hofstadter Model

Alexander Lau,[1,*] Carmine Ortix,[1,2] and Jeroen van den Brink[1,3]
[1]Institute for Theoretical Solid State Physics, IFW Dresden, 01171 Dresden, Germany
[2]Institute for Theoretical Physics, Center for Extreme Matter and Emergent Phenomena, Utrecht University, Leuvenlaan 4, 3584 CE Utrecht, Netherlands
[3]Department of Physics, TU Dresden, 01062 Dresden, Germany
(Received 2 July 2015; published 20 November 2015)

The Hofstadter model is a simple yet powerful Hamiltonian to study quantum Hall physics in a lattice system, manifesting its essential topological states. Lattice dimerization in the Hofstadter model opens an energy gap at half filling. Here we show that even if the ensuing insulator has a Chern number equal to *zero*, concomitantly a doublet of edge states appear that are pinned at specific momenta. We demonstrate that these states are topologically protected by inversion symmetry in specific one-dimensional cuts in momentum space, define and calculate the corresponding invariants, and identify a platform for the experimental detection of these novel topological states.

DOI: 10.1103/PhysRevLett.115.216805 PACS numbers: 73.43.-f, 03.65.Vf, 42.70.Qs, 73.21.Cd

Introduction.—Since the discovery of the quantum Hall effect in 1980 [1], and its theoretical explanation in terms of the topological properties of the Landau levels [2,3], the investigation of topological phases of matter has become a most active research area. It has brought forth the theoretical prediction and experimental verification of a plethora of different topologically nontrivial electronic quantum phases [4–11]. Contrary to their trivial counterparts, topologically nontrivial quantum phases exhibit protected surface or edge states that are inside the bulk gap. These topological states are a direct physical consequence of the topology of the bulk band structure which is characterized by a quantized topological invariant [12,13]. One of the most celebrated models for the study of topological properties of matter was introduced by Hofstadter in 1976 [14]. It describes tight-binding electrons on a rectangular lattice in the presence of a uniform magnetic field and allows the study of the quantum Hall effect on a lattice. Indeed, the Hofstadter Hamiltonian harbors the topological chiral edge states that are responsible for the quantized Hall conductivity. If the system is perturbed, the quantization stays intact and precise, even if the perturbation introduces additional edge states: any pair of accidentally induced edge states has opposite chirality and therefore yields an exactly zero contribution to the Hall conductivity, which causes the robustness of the quantum Hall effect.

In this Letter we show that in spite of this seemingly benign perturbation to the Hofstadter Hamiltonian, a moderate lattice dimerization causes a topological phase transition, spawning counterpropagating edge states not contributing to the Hall conductivity that are yet topologically protected. We show that the presence of these states can be understood from the topological properties of lower-dimensional cuts of the system, using a mapping of the Hofstadter Hamiltonian on a collection of one-dimensional Aubry-André-Harper (AAH) models [15,16]. A subset of AAH chains in this collection preserves inversion symmetry, which guarantees the presence of globally topologically protected doublets of end modes to which the edge states are pinned. Such end modes are different in nature from the topological edge states found in the context of off-diagonal AAH models [17]. To explicitly prove the robustness of the emerging edge states, we define and calculate the topological invariant that protects them, which turns out to be an invariant for inversion-symmetric AAH models. Our results thus add a new chapter to the successful history of analogies between Hofstadter and AAH models [17–21]. Finally, we also identify an experimental setup to probe the existence and properties of these new topological edge states.

Dimerized hofstadter model—The Hofstadter model [14] describes spinless electrons on a rectangular lattice with lattice constants a and b subject to a perpendicular magnetic field. In addition, we consider the possibility of a lattice dimerization along one direction being present, which leads to a modulation of hopping amplitudes as indicated in Fig. 1. For simplicity, we neglect a modulation of the magnetic fluxes, which would be present in a realistic system due to the change of the lattice parameter a. However, we assure the reader that such a modulation leads to the same general results [22]. The corresponding tight-binding Hamiltonian, adopting the Landau gauge in a mixed momentum-position space as obtained by performing a Fourier transformation only along the "undimerized" direction y, reads

$$\mathcal{H} = \sum_{j_x,k_y} [t_x - (-1)^{j_x}\delta t](c^\dagger_{j_x+1,k_y} c_{j_x,k_y} + c^\dagger_{j_x-1,k_y} c_{j_x,k_y}) + \sum_{j_x,k_y} 2t_y \cos(bk_y + 2\pi\alpha j_x) c^\dagger_{j_x,k_y} c_{j_x,k_y}, \quad (1)$$

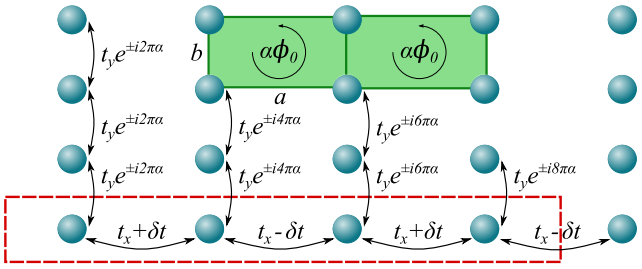

FIG. 1 (color online). Scheme of the hopping amplitudes in the dimerized Hofstadter model in the Landau gauge. All plaquettes of size $a \times b$, partially indicated by green rectangles, are penetrated by a magnetic flux of $\phi = \alpha\phi_0$, where $\phi_0 = hc/e$ is a magnetic flux quantum. In addition, we show a magnetic unit cell for the case $\alpha = 1/4$ (red dashed rectangle). Note that the unit cell is penetrated by exactly one flux quantum ϕ_0.

where $c^{\dagger}_{j_x,j_y}$, c_{j_x,j_y} are fermionic creation and annihilation operators, α is the magnetic flux in units of the magnetic flux quantum ϕ_0 penetrating each plaquette of size $a \times b$, $t_{x,y}$ are the nearest-neighbor (average) hopping amplitudes while δt parametrizes the dimerization strength. For simplicity, we will restrict ourselves to the case for which $\alpha = 1/4$ from here on, but it should be pointed out that the final results are general and hold also for other values of the magnetic flux [22]. The magnetic unit cell of the $\alpha = 1/4$ dimerized Hofstadter model contains four inequivalent lattice sites (cf. Fig. 1). Therefore, the corresponding Bloch Hamiltonian in full momentum space can be written in terms of the Dirac matrices Γ_i and their commutators Γ_{ij} [24]. For a unit cell going from $j_x = 1$ to $j_x = 4$, the Hamiltonian reads

$$\begin{aligned} H = {} & t_y(\cos bk_y - \sin bk_y)\Gamma_5 + t_y(\cos bk_y + \sin bk_y)\Gamma_{21} \\ & (t_x + \delta t)\Gamma_{45} + \frac{1}{2}(t_x - \delta t)(1 - \cos 4ak_x)\Gamma_{41} \\ & + \frac{1}{2}(t_x - \delta t)(1 + \cos 4ak_x)\Gamma_{23} \\ & - \frac{1}{2}(t_x - \delta t)\sin 4ak_x(\Gamma_{24} + \Gamma_{31}). \end{aligned} \tag{2}$$

Since the prime physical consequence of nontrivial topological states is the existence of chiral edge states, we study the dimerized Hofstadter model in a ribbon geometry with periodic boundary conditions in the y direction and open boundary conditions with a finite number of magnetic unit cells N_x in the x direction. Thus, the ribbon with $\alpha = 1/4$ is of width $W = 4N_x a$ and terminated by two boundaries perpendicular to the dimerization direction. The band structure of the ribbon is then determined via exact diagonalization of the first-quantized $4L \times 4L$ Hamiltonian corresponding to Eq. (1). Figure 2 shows the ensuing band structure for $t_y = t_x/2$.

In the absence of dimerization the bulk spectrum is gapped for filling fractions $1/4$ and $3/4$, but gapless at half filling with four bulk Dirac points. This is the usual situation of the Hofstadter spectrum with magnetic flux ratio $\alpha = p/q$, with p, $q \in \mathbb{N}$ and $q = 2r$ even [14,25]: there are $q - 2$ bulk energy gaps, whereas the two central bands have q touching points at $E = 0$. Furthermore, within each bulk energy gap we observe one pair of counterpropagating edge states traversing the bulk gap localized at the edges of the system. Those can be attributed to the nontrivial bulk topology for the corresponding filling levels by bulk-boundary correspondence. Indeed, a calculation of the Chern number n_l [2,3] for each energy band l yields Hall conductivities $\sigma = \sum_{l \in \mathrm{occ.}} n_l$ of $\sigma(1/4) = -1$ and $\sigma(3/4) = +1$. This gives rise to one topologically protected state per edge, consistent with the so-called Diophantine equation [25].

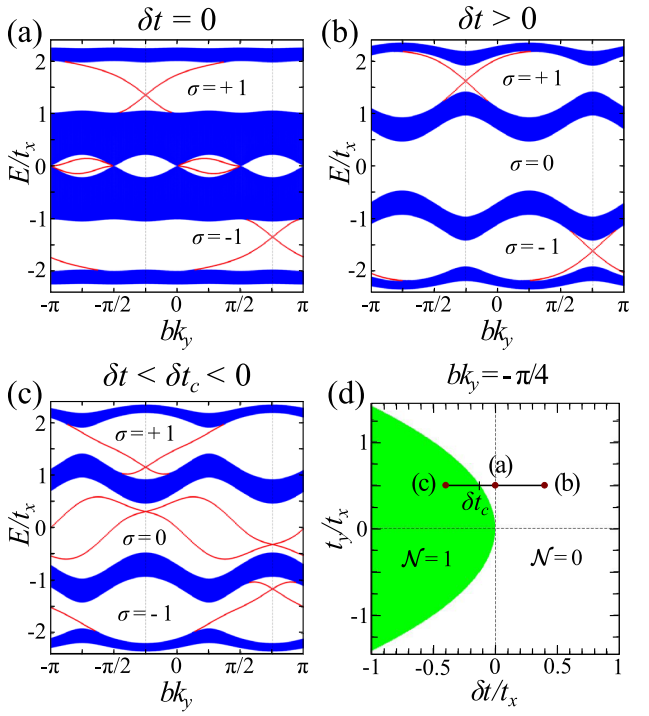

FIG. 2 (color online). Band structures for the dimerized Hofstadter model in a ribbon geometry of width $W = 4N_x a$: $\alpha = 1/4$, $N_x = 100$. Parameters are (in units of t_x) (a) $t_y = 0.5$, $\delta t = 0$ (no dimerization), (b) $t_y = 0.5$, $\delta t = 0.4$ (trivial dimerization), (c) $t_y = 0.5$, $\delta t = -0.4$ (nontrivial dimerization). States localized at the edges of the system are highlighted in red. Hall conductivities σ for Fermi levels inside the bulk energy gaps are displayed in units of e^2/h. Relevant inversion-symmetric AAH cuts are indicated by dashed vertical lines. Note that in (c) there are nontrivial edge states at half filling although the corresponding Hall conductivity is zero. To explain this, we show in (d) a half-filling t_y-δt phase diagram for the inversion-symmetric AAH model with $k_y b = -\pi/4$ and with respect to the 1D invariant $\mathcal{N}$ of Eq. (3). Points corresponding to (a)–(c) are indicated by red circles, including a possible path connecting them.

For a finite dimerization mass $\delta t > 0$, the modulated hopping amplitude acts as a gap-opening perturbation at half filling, yielding an additional insulating phase for

which we calculate a trivial Hall conductivity of $\sigma(1/2) = 0$. Hence, topologically protected edge states are not expected for this phase. Indeed, the two additional bands of edge states between the touching points of the two central bands of Fig. 2(a) are pushed into the bulk continuum and localized in-gap states are absent [see Fig. 2(b)]. Moreover, the edge states of the nontrivial insulating states are only slightly deformed, signaling that the dimerization mass does not interfere with the bulk topological properties of the system.

The situation for $\delta t < 0$ turns out to be much richer. For small values of the dimerization mass, one again observes the opening of a bulk gap at half filling. However, at a critical value $\delta t = \delta t_c < 0$ [see Fig. 2(d) for a phase diagram], a pair of gap closing and reopening points appears at $bk_y = -\pi/4$ and $bk_y = 3\pi/4$. Furthermore, in close proximity to these points, a pair of counterpropagating chiral edge states [Fig. 2(c)] is revealed. This is in agreement with the vanishing Hall conductivity since their contribution to the Hall current is exactly opposite. By further increasing the dimerization, the corresponding edge bands are deformed. However, the doublets of in-gap edge states remain pinned at the momenta $bk_y = -\pi/4$, $3\pi/4$ and cannot be pushed into the bulk *independent* of the value of δt and t_y.

We now show that the presence of such doublets of half-filling in-gap edge states has a topological origin. In the form of Eq. (1), the dimerized Hofstadter model can be viewed as a collection of dimerized 1D chains parametrized by the momentum k_y, with periodically modulated on-site potentials of periodicity $1/\alpha$, amplitude $2t_y$, and phase bk_y. These chains are equivalent to a specific combination of diagonal and off-diagonal AAH models [17,18,20,21]. AAH models have been the subject of intensive research because of their correspondence to a number of fundamental models, such as 2D lattice models with magnetic flux [20], the Kitaev model [26], or the Su-Schrieffer-Heeger model [27]. Note that the specific form of AAH models studied here is different from other studies in the literature. For any value of k_y the AAH models possess time-reversal symmetry with $T = K$, $k_x \to -k_x$, and with $T^2 = +1$, where K is complex conjugation. Moreover, for $\alpha = 1/4$ the 1D Hamiltonians preserve inversion symmetry for four distinct values of k_y. In general, one can show that all dimerized Hofstadter models with rational $\alpha = p/q$ possess at least two and at most $2q$ distinct inversion-symmetric cuts [22]. Note that for a finite number of magnetic unit cells with open boundary conditions along the x direction, inversion symmetry persists only in *two* of these chains. In our example, those cuts are at $k_y b = -\pi/4$ or $3\pi/4$, with the 1D parity operator described by $P = \sigma^x \otimes \tau^x$, σ^i and τ^i being Pauli matrices.

One-dimensional topological invariants.—The effective 1D inversion-symmetric AAH Hamiltonians fall into the orthogonal class (AI) with inversion symmetry of topological insulators with additional point-group symmetries introduced by Lu and Lee [28] who thereby extend the famous Altland-Zirnbauer (AZ) table [13,29–33]. Note that class AI of the original AZ table is trivial in 1D. Since inversion operator P ($P^2 = +1$) and time-reversal operator T ($T^2 = +1$) commute, the 1D Hamiltonians allow for a $\mathbb{Z}$ topological invariant. Such an integer invariant can be defined as follows [34]. Let us consider a 1D system on a chain with inversion symmetry described by the Bloch Hamiltonian $H(k)$, $k \in (-\pi/a, \pi/a]$. Inversion symmetry implies $P^{-1}H(k)P = H(-k)$, where P is a matrix representation of inversion. In particular, $H(k)$ commutes with P at inversion-invariant momenta. Thus, eigenstates of $H(k)$ have a well-defined parity $\zeta_i(k_{\mathrm{inv}}) = \pm 1$ at those points. The eigenvalues of an operator cannot be changed by continuous deformations of the Hamiltonian, up to the order. However, a change of the order is only possible by closing and reopening the energy gap between two states. For a 1D inversion-symmetric system, an integer invariant is therefore defined by [34],

$$\mathcal{N} := |n_1 - n_2|, \tag{3}$$

where n_1 and n_2 are the number of negative parities at $k = 0$ and $k = \pi/a$, respectively.

Let us now apply this to the inversion-symmetric AAH cuts of our exemplary system. In Fig. 3, we show 1D bulk spectra of the inversion-symmetric cuts corresponding to Fig. 2 for different values of the dimerization mass.

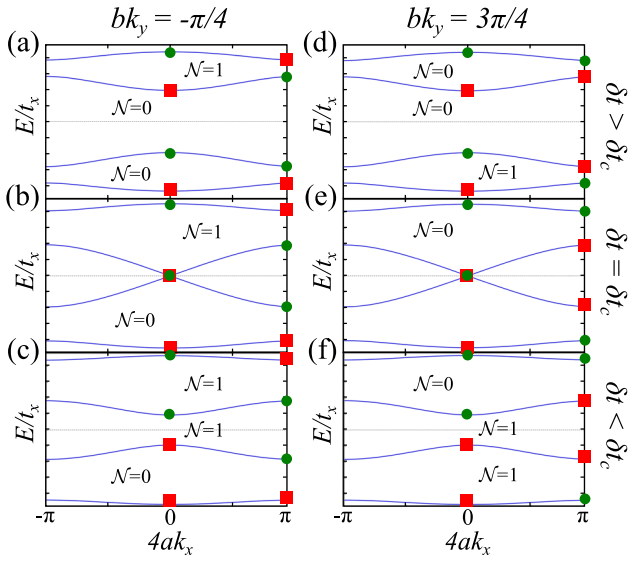

FIG. 3 (color online). Bulk band structures for inversion-symmetric AAH models with and without dimerization: $\alpha = 1/4$, $t_y = 0.5t_x$; $\delta t = 0.4t_x$ in (a) and (d), $\delta t = \delta t_c = -1/8t_x$ in (b) and (e), $\delta t = -0.4t_x$ in (c) and (f). The parities at the inversion-invariant momenta $k_x = 0$ and $\pi/4a$ are indicated by green circles ($\zeta = +1$) and red squares ($\zeta = -1$). We also display the topological invariants $\mathcal{N}$ corresponding to Fermi levels inside the respective bulk energy gaps.

Furthermore, we display the parities of the bulk states at the inversion-invariant momenta $k_x = 0$ and $k_x = \pi/4a$. This enables us to calculate the topological invariant $\mathcal{N}$.

As an example, we discuss the results for $bk_y = -\pi/4$ and $t_y > 0$ [see Figs. 3(a)–3(c)]. Independent of the dimerization mass, we find $\mathcal{N} = 1$ for $3/4$ filling and $\mathcal{N} = 0$ for $1/4$ filling. This means the system is topologically nontrivial with one pair of degenerate end modes if the Fermi level is in the upper gap. On the contrary, we have a trivial system without end modes for $1/4$ filling. Going back to the full Hofstadter model, this explains why the crossing of the $3/4$ filling quantum Hall edge states is pinned to the point $bk_y = -\pi/4$.

For half filling, the situation is more subtle. For $\delta t > \delta t_c$, our calculations yield $\mathcal{N} = 0$, rendering the system topologically trivial. Indeed, we do not observe end modes in this case. In contrast to that, for $\delta t < \delta t_c$ the system is topologically nontrivial with $\mathcal{N} = 1$ and we find a pair of degenerate end modes in the finite system. The reason for this is that the $k_x = 0$ parities of the two central bands are switched while going from $\delta t > \delta t_c$ to $\delta t < t_c$—a band inversion takes place.

This explicitly explains the observed pinning of the degenerate edge states of the dimerized Hofstadter model at half filling. They are protected by inversion symmetry in specific 1D cuts corresponding to topologically nontrival inversion-symmetric AAH models. The corresponding Hall conductivity is zero.

We remark that the qualitative results do not depend on the choice of the unit cell or on how the system is terminated, as long as there is at least one underlying AAH chain with inversion symmetry. This is always the case for an even number of lattice sites in the direction of dimerization, whereas for an odd number of sites inversion symmetry is lost in *all* dimerized AAH chains [22]. However, the details, in particular the position of the inversion-symmetric cuts, might change.

Furthermore, note that the role of the sign of δt does depend on the termination of the system, which is the usual situation for dimerized systems such as the Su-Schrieffer-Heeger model. More specifically, the sign of δt is reversed if we consider a dimerized Hofstadter ribbon with unit cells shifted by one lattice site in the dimerization direction. Physically, this only reflects the fact that the last bonds on both sides of the ribbon must be weaker than the average bond strength to get nontrivial localized states.

Experimental detection.—The Hofstadter model and the AAH model, respectively, have been realized in different experimental setups such as ultracold atoms in optical lattices [35,36] or photonic crystals [19,37]. These experimental platforms are characterized by an exceptional tunability which brings a much wider range of accessible model parameters into reach. A very promising route towards the experimental detection of the pinned degenerate topological states would be the realization of the inversion-symmetric AAH models. Similar to the setups described in Refs. [17] and [19], a periodic lattice of coupled single-mode waveguides can be prepared on a two-dimensional substrate, where each waveguide corresponds to a lattice site of the finite 1D AAH model. The small spacing between waveguides allows a light wave, propagating through one of the guides, to tunnel between neighboring waveguides, thereby simulating a hopping process. Furthermore, the width of a waveguide determines the propagation properties of a light wave, which is used to simulate and vary the on-site potentials for different lattice sites. In this way, all the model parameters of Eq. (1) could be implemented and adjusted. By injecting light into one of the outermost (boundary) waveguides and by measuring the outgoing intensity distribution, the localized and topologically protected end states could then be detected directly.

Conclusions.—We have shown that, depending on the sign of the dimerization mass δt and on the position of the boundaries, the dimerized Hofstadter model exhibits topologically protected edge states at half filling. The topological states propagate along the edges of a ribbon, perpendicular to the dimerization direction, whose width must be chosen to extend over an even number of lattice sites. This has been confirmed by numerical calculations for a model with an exemplary value of the magnetic flux and generalizes to arbitrary rational values. The edge states are protected by 1D inversion symmetry in specific cuts of the two-dimensional Hofstadter Brillouin zone corresponding to inversion-symmetric AAH models. Most importantly, they are different from the well-known quantum-Hall edge states because their Hall conductivity is zero and they are, thus, protected solely by inversion symmetry. Moreover, the associated edge bands can be completely disconnected from the bulk continuum of bands. To uncover the topological nature of the edge states, we have defined and calculated the integer topological invariant for the 1D inversion-symmetric cuts, which fall in class AI of the extended classification scheme by Lu and Lee [28]. These states are thus fundamentally different from those in the purely off-diagonal AAH model [17], which is in the *standard* chiral orthogonal AZ class (BDI).

We have further proposed an experimental setup based on a lattice of coupled single-mode waveguides that allows for the direct detection of the novel topological states we predict.

From a more general perspective, we have presented a two-dimensional insulating system where lower-dimensional, 1D physics enriches the global topological structure of the system. Going one step further, it will be very interesting to find realistic materials featuring the ensuing zero-Hall-conductivity topological edge states protected in a reduced dimension.

C. O. acknowledges the financial support of the Future and Emerging Technologies (FET) program within the

Seventh Framework Programme for Research of the European Commission, under FET-Open Grant No. 618083 (CNTQC), and also the support of the Deutsche Forschungsgemeinschaft (Grant No. OR 404/1-1). We thank SFB 1143 for support.

*Corresponding author.
a.lau@ifw-dresden.de

[1] K. v. Klitzing, G. Dorda, and M. Pepper, Phys. Rev. Lett. **45**, 494 (1980).
[2] D. J. Thouless, M. Kohmoto, M. P. Nightingale, and M. den Nijs, Phys. Rev. Lett. **49**, 405 (1982).
[3] M. Kohmoto, Ann. Phys. (N.Y.) **160**, 343 (1985).
[4] B. A. Bernevig, T. L. Hughes, and S.-C. Zhang, Science **314**, 1757 (2006).
[5] M. König, S. Wiedmann, C. Brüne, A. Roth, H. Buhmann, L. W. Molenkamp, X.-L. Qi, and S.-C. Zhang, Science **318**, 766 (2007).
[6] D. Hsieh, Y. Xia, L. Wray, D. Qian, A. Pal, J. H. Dil, J. Osterwalder, F. Meier, G. Bihlmayer, C. L. Kane, Y. S. Hor, R. J. Cava, and M. Z. Hasan, Science **323**, 919 (2009).
[7] B. Rasche, A. Isaeva, M. Ruck, S. Borisenko, V. Zabolotnyy, B. Büchner, K. Koepernik, C. Ortix, M. Richter, and J. van den Brink, Nat. Mater. **12**, 422 (2013).
[8] C. Pauly, B. Rasche, K. Koepernik, M. Liebmann, M. Pratzer, M. Richter, J. Kellner, M. Eschbach, B. Kaufmann, L. Plucinski, C. M. Schneider, M. Ruck, J. van den Brink, and M. Morgenstern, Nat. Phys. **11**, 338 (2015).
[9] C. L. Kane and E. J. Mele, Phys. Rev. Lett. **95**, 226801 (2005).
[10] C.-C. Liu, W. Feng, and Y. Yao, Phys. Rev. Lett. **107**, 076802 (2011).
[11] A. Lau and C. Timm, Phys. Rev. B **88**, 165402 (2013).
[12] M. Z. Hasan and C. L. Kane, Rev. Mod. Phys. **82**, 3045 (2010).
[13] S. Ryu, A. P. Schnyder, A. Furusaki, and A. W. W. Ludwig, New J. Phys. **12**, 065010 (2010).
[14] D. R. Hofstadter, Phys. Rev. B **14**, 2239 (1976).
[15] S. Aubry and G. André, Ann. Isr. Phys. Soc. **3**, 133 (1980).
[16] P. G. Harper, Proc. Phys. Soc. London Sect. A **68**, 874 (1955).
[17] S. Ganeshan, K. Sun, and S. Das Sarma, Phys. Rev. Lett. **110**, 180403 (2013).
[18] L.-J. Lang, X. Cai, and S. Chen, Phys. Rev. Lett. **108**, 220401 (2012).
[19] Y. E. Kraus, Y. Lahini, Z. Ringel, M. Verbin, and O. Zilberberg, Phys. Rev. Lett. **109**, 106402 (2012).
[20] Y. E. Kraus and O. Zilberberg, Phys. Rev. Lett. **109**, 116404 (2012).
[21] P. Marra, R. Citro, and C. Ortix, Phys. Rev. B **91**, 125411 (2015).
[22] See Supplemental Material at http://link.aps.org/supplemental/10.1103/PhysRevLett.115.216805, which includes Ref. [23], for a derivation of the inversion-symmetric cuts, for dimerized Hofstadter models with other values of the magnetic flux, and for a discussion of the effects of a flux modulation.
[23] M. Ezawa, Y. Tanaka, and N. Nagaosa, Sci. Rep. **3**, 2790 (2013).
[24] L. Fu and C. L. Kane, Phys. Rev. B **76**, 045302 (2007).
[25] D. Osadchy and J. E. Avron, J. Math. Phys. (N.Y.) **42**, 5665 (2001).
[26] A. Y. Kitaev, Phys. Usp. **44**, 131 (2001).
[27] W. P. Su, J. R. Schrieffer, and A. J. Heeger, Phys. Rev. Lett. **42**, 1698 (1979).
[28] Y.-M. Lu and D.-H. Lee, arXiv:1403.5558.
[29] M. R. Zirnbauer, J. Math. Phys. (N.Y.) **37**, 4986 (1996).
[30] A. Altland and M. R. Zirnbauer, Phys. Rev. B **55**, 1142 (1997).
[31] P. Heinzner, A. Huckleberry, and M. R. Zirnbauer, Commun. Math. Phys. **257**, 725 (2005).
[32] A. P. Schnyder, S. Ryu, A. Furusaki, and A. W. W. Ludwig, Phys. Rev. B **78**, 195125 (2008).
[33] A. Kitaev, AIP Conf. Proc. **1134**, 22 (2009).
[34] T. L. Hughes, E. Prodan, and B. A. Bernevig, Phys. Rev. B **83**, 245132 (2011).
[35] M. Aidelsburger, M. Atala, M. Lohse, J. T. Barreiro, B. Paredes, and I. Bloch, Phys. Rev. Lett. **111**, 185301 (2013).
[36] H. Miyake, G. A. Siviloglou, C. J. Kennedy, W. C. Burton, and W. Ketterle, Phys. Rev. Lett. **111**, 185302 (2013).
[37] Y. Lahini, R. Pugatch, F. Pozzi, M. Sorel, R. Morandotti, N. Davidson, and Y. Silberberg, Phys. Rev. Lett. **103**, 013901 (2009).